Growth of zinc phosphate coatings on AZ91D magnesium alloy

G.Y. Li, J.S. Lian *, L.Y. Niu, Z.H. Jiang, Q. Jiang

Key Laboratory of Automobile Materials, Ministry of Education, China, College of Materials Science and Engineering, Jilin University, Nanling Campus, Changchun, l30025, China

Abstract

Zinc phosphate coating was formed on AZ91D magnesium alloy through a phosphating bath where H_3PO_4, ZnO, $Zn(NO_3)_2$ and NaF were applied. Chlorate ($NaClO_3$) was used as an accelerator of phosphatization to replace nitrite. The coating compositions were hopeite ($Zn_3(PO_4)_2 \cdot 4H_2O$) and Zn. The growth process of the phosphate film on the magnesium alloy substrate was investigated by SEM observation and XRD analysis. In the early stage (0–60 s) of phosphatization, both hopeite and metallic zinc nucleated and grew together on the substrate to form flower structure. A great number and uniform nucleation of hopeite and metallic zinc implied that they formed on the β and α phases of the AZ91D magnesium alloy simultaneously. Afterwards, because magnesium alloy substrate was almost fully covered, only hopeite deposited continuously to form slab-like structure. The formed zinc phosphate coatings exhibited high corrosion resistance in 5% NaCl solution as shown by polarization measurement.
© 2006 Elsevier B.V. All rights reserved.

Keywords: Zinc phosphate coating; Magnesium alloy; Corrosion resistance

1. Introduction

Magnesium alloy has some advantageous properties including low density and high strength/weight ratio, high thermal conductivity, very good electromagnetic features and being easily recycled. These properties make it valuable in a number of industrial fields including automobile, aerospace components, mobile phones and sporting goods [1–6]. However, the application of magnesium alloys has been limited due to their undesirable properties including poor corrosion and low wear resistance. A more effective way to prevent corrosion of magnesium alloys is to coat the substrate materials [2].

Surface treatments, such as the formation of conversion coatings, are commonly applied to magnesium alloys in order to increase the corrosion resistance. Recently, some surface protection reports of conversion coatings on magnesium alloys were published including chromate conversion coating [7,8]. Phosphate technique has been used to steel, aluminum

alloy and titanium alloy as protective coating or pretreatment to underneath the paint [9–13]. In fact, phosphating may be a promising method for magnesium alloys anticorrosion and pretreatment process before paint, tends to replace chromate treatment where the environment polluted hexad chromium was involved. There were a few researches of phosphate films on magnesium alloys recently [14,15]. Kouisni et al. [14] studied the formation and growth of zinc phosphate film on an AM60 magnesium alloy. The influence of zinc ions (Zn^{2+}) and nitrate on the phosphating process and mechanism were investigated. In a previous work, a phosphating bath contained mainly ZnO, H_3PO_4 and NaF was employed to obtain zinc phosphate conversion coatings on AZ91D magnesium alloy [15]. In these studies of phosphating on magnesium alloys [14,15], nitrate and nitrite were used as the accelerating agents that were added in the phosphating bath. However, nitrite is a carcinogen that should be abandoned to use. It has been shown that the addition of metal saline in the phosphating bath can greatly influence the microstructure of phosphate coating and made the coating more dense and fine [9].

In the present study, a phosphating bath containing H_3PO_4, ZnO, $ZnNO_3$ and NaF was applied to form phosphate coating

* Corresponding author. Fax: +86 431 5095876.
  E-mail address: lianjs@jlu.edu.cn (J.S. Lian).

Table 1
The compositions of AZ91D magnesium alloy (in wt.%)

Al	Zn	Mn	Ni	Cu	Ca	Si	K	Fe	Magnesium
8.77	0.74	0.l8	0.00l	0.00l	<0.0l	<0.0l	<0.0l	0.00l	Balance

on AZ91D magnesium alloy. Chlorate ($NaClO_3$) was used as an accelerator agent of phosphatization to replace nitrite. The addition of $NaClO_3$ will greatly influence the microstructure of phosphate coating. The phosphating mechanism was discussed. Because there is also metallic zinc in the coating, the growth process and phosphating mechanism was investigated detailedly by means of SEM, EDS and XRD. The corrosion resistance of the coating was estimated by the time-potential curve and polarization curves.

2. Experiments

AZ91D die-casting magnesium alloy samples with the specimen size of $50 \times 50 \times 3$ mm were used as substrate materials. The compositions of the alloy are given in Table l. The samples were grinded using No. l500 sand papers and degreased in 10% KOH at 60 °C and rinsed in de-ionized water to remove all the alkali before the zinc phosphating treatment. The cleaned specimens were then treated in the phosphating bath and were dried. The ingredients of the zinc phosphating bath were shown in Table 2. The pH of the bath was adjusted by H_3PO_4 or $NH_3 \cdot H_2O$ to around 2.4. The phosphating temperature was 40–45 °C.

The nucleation and growth of the phosphate coating was observed with the SEM. The phases in the phosphate coatings were analyzed by XRD (D/max-2500PC, CuKα). The weight of the phosphate coating was measured by the method described in Ref. [15]. The open circuit potential of the phosphate-coated specimens at different phosphating time was measured. A saturated calomel electrode (SCE) was used as a reference electrode. Potentials were recorded from the beginning of phosphating to about 180 s by immersing the working electrode in the phosphating bath.

The polarization measurement of the specimens with phosphate coating was conducted in a 5% NaCl solution. Three-electrode cell configurations were employed for the polarization measurements. The counter electrode was a platinum plate. Saturated calomel electrode (SCE) was applied as a reference electrode. The reference electrode was placed outside the cell and connected to the specimen surface by a Luggin capillary and a salt bridge. All polarizations were carried out using a computer-controlled SF M273 potentiostat of EG and G. The current was recorded as the potential increased at a scan rate of 50 mV.

3. Results and discussion

3.1. Phosphating reactions mechanism

In the present phosphating process, both ZnO and $Zn(NO_3)_2$ were added in the bath, which is different from the previous

studies [14,15]. ZnO reacted with H_3PO_4 to form $Zn(H_2PO_4)_2 \cdot 2H_2O$:

$$ZnO + 2H_3PO_4 + H_2O \rightarrow Zn(H_2PO_4)_2 \cdot 2H_2O \quad (1)$$
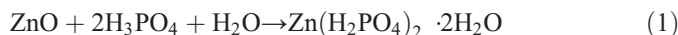
The product $Zn(H_2PO_4)_2 2H_2O$ of reaction (1) is soluble and it dissolved in the solution to produce:

$$Zn(H_2PO_4)_2 \cdot 2H_2O \Leftrightarrow ZnPO_4^- + H_2PO_4^- + 2H^+ + 2H_2O \quad (2)$$
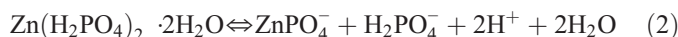
The complex ion $ZnPO_4^-$ has the ionization reaction as follow:

$$ZnPO_4^- \Leftrightarrow Zn^{2+} + PO_4^{3-} \quad (3)$$

In the phosphating bath, $Zn(NO_3)_2$ has two actions. First, it provides Zn^{2+} in the solution:

$$Zn(NO_3)_2 \rightarrow Zn^{2+} + 2NO_3^- \quad (4)$$
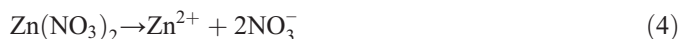
Then the NO_3^- ions can accelerate the deposition of $Zn_3(PO_4)_2 4H_2O$ (see Eq. (10)).

During phosphatization, as soon as the alloy sample is soaked in the phosphating bath, the surface of sample divided into micro anode sites (lower electron density sites) and micro cathode sites (higher electron density sites) and the reactions on the surfaces should be thought to take place on different local polarization sites correspondingly. As to the AZ91D magnesium alloy, finer β ($Mg_{17}Al_{12}$) phases distribute uniformly on magnesium matrix [16], and β phase in the magnesium alloys is regarded as the micro cathode sites [13] and magnesium the micro anode sites. It has been reported that there are a lot of magnesium atoms and some aluminum atoms that resolved at the micro anode sites in the Mg–Al–Zn alloy surfaces and there are no resolved zinc atoms [17]. Therefore, the following reactions can occur at micro-anode sites. Magnesium dissolved and releases metal ions at the micro anode sites:

$$Mg \rightarrow Mg^{2+} + 2e \quad (5)$$
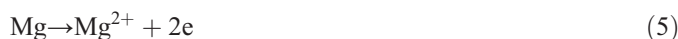
There is also a small quantity of aluminum dissolved into the bath:

$$Al \rightarrow Al^{3+} + 3e \quad (6)$$

Because of the difference in the standard potential of zinc (−1.76 V) and magnesium (−2.36 V), Mg on magnesium alloy surface dissolved in bath to give out electrons, which reduced some Zn^{2+} near the surface to Zn deposited on the

Table 2
The compositions of phosphating bath

Composition	Concentration (mol/L)
Phosphoric acid	0.065
Zinc oxide	0.029
Sodium fluoride	0.040
Zinc nitrate	0.102
Sodium chlorate	0.028
Organic amine	0.007
Ammonia	0.034

surface on the micro cathode sites of some α phases (see Sec. 3.2) and become the composition of the phosphate coating:

$$Zn^{2+} + 2e \rightarrow Zn\downarrow \qquad (7)$$

At the micro cathode sites hydrogen ions were reduced simultaneously:

$$2H^+ + 2e \rightarrow H_2 \qquad (8)$$

The reduction of the hydrogen ions results in the increase of local pH at the metal-bath interface, which facilitated the

precipitation of insoluble zinc phosphate [14,15]. The formation of insoluble phosphate film may have followed the reaction:

$$3Zn^{+2} + 2H_2PO_4^- + 4H_2O + 4e \rightarrow Zn_3(PO_4)_2 \cdot 4H_2O + 2H_2 \qquad (9)$$
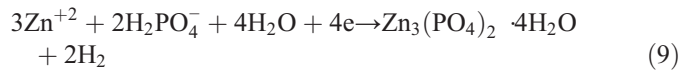
Here $Zn_3(PO_4)_2$ $4H_2O$ is the main ingredient of the phosphate film. After the original phosphate film has formed it is still regarded as the micro cathode. Reaction (9) progresses continuously, until the nucleation and growth of phosphate crystals to form the integrated phosphate film and all of the micro anodes are covered. There should be metallic zinc crystals in the
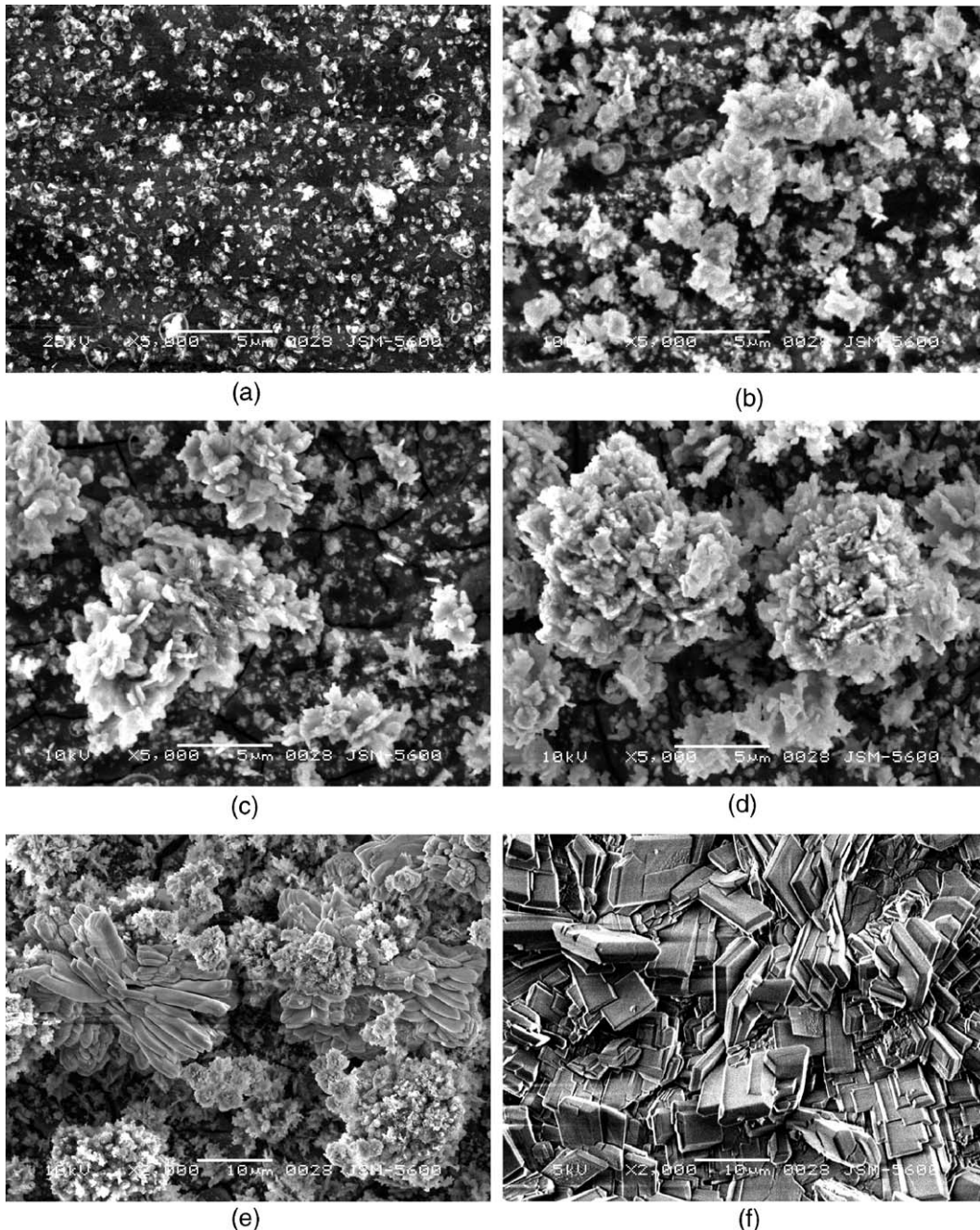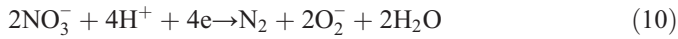

Fig. 1. SEM images of the zinc phosphate coating on the AZ91D magnesium alloy: (a) 1.5 s, (b) 5 s, (c) 10 s, (d) 30 s, (e) 60 s, (f) 180 s, after immersion in the phosphating bath.

zinc phosphate coating due to the reaction of Eq. (7). This is different from the traditional zinc phosphate coating on steel.

In the present research, chlorate (NaClO$_3$) was used as accelerator to replace nitrite because the latter is harmful to human beings. That is, both nitrate (Zn(NO$_3$)$_2$) and chlorate (NaClO$_3$) were used in the phosphating process. During phosphating, the NO$_3^-$ ions reacts with hydrogen ions:

$$2NO_3^- + 4H^+ + 4e \rightarrow N_2 + 2O_2^- + 2H_2O \qquad (10)$$

This reaction consumes hydrogen ions and makes the pH of the bath near the magnesium alloy surface rise rapidly and it is beneficial to the formation of phosphate coating [14,15]. Similarly, NaClO$_3$ dissolved in the solution to give out ClO$_3^-$ ions, which consumed hydrogen ions produced in the phosphating reaction and accelerate the phosphating reaction:

$$ClO_3^- + 6H^+ + 6e \rightarrow Cl^- + 3H_2O \qquad (11)$$
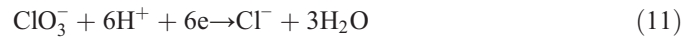
3.2. The growth of the phosphating coating

Fig. 1 shows the surface morphology (×5000) of the phosphate films on the magnesium alloy at different phosphating
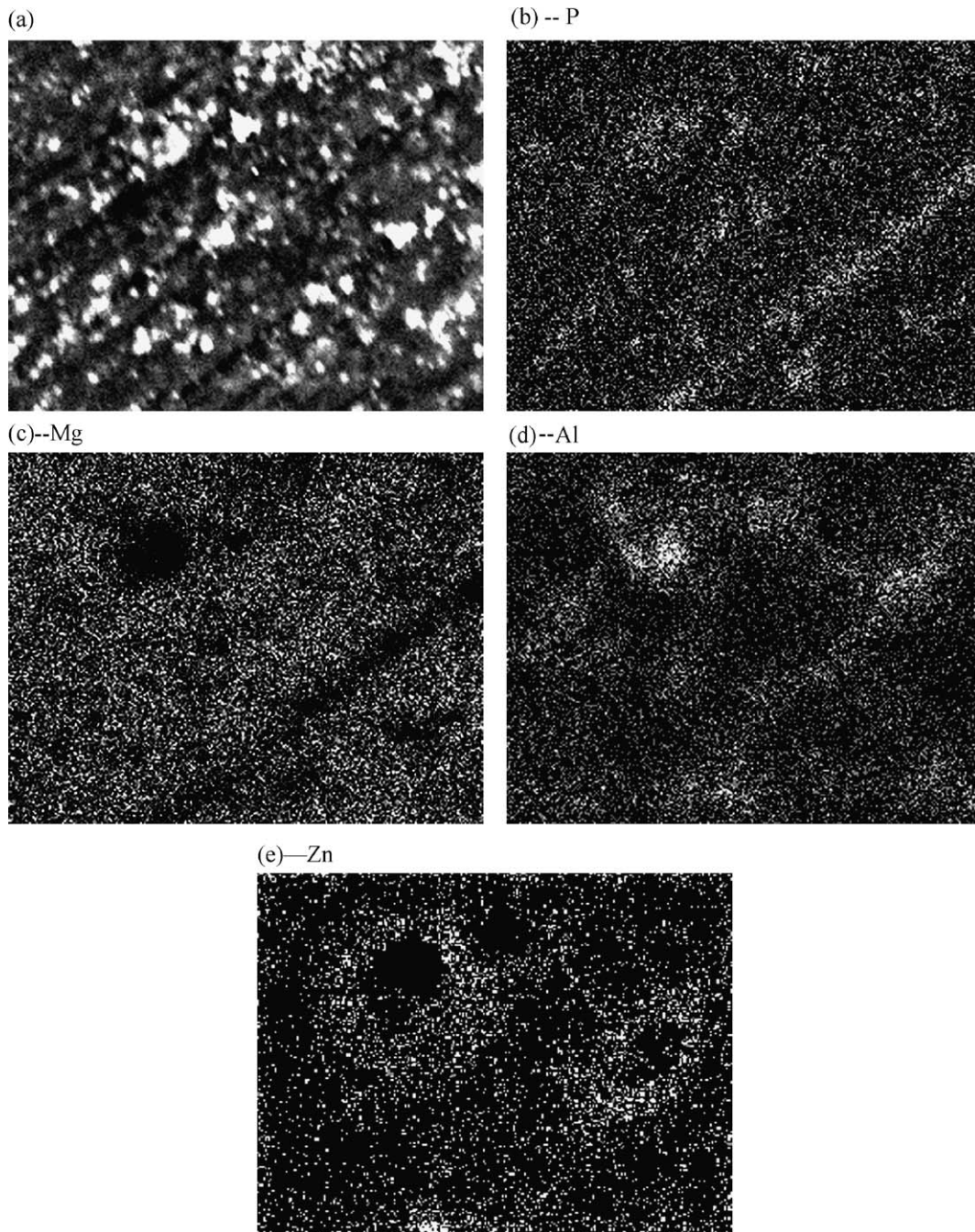

Fig. 2. SEM images and energy spectrum images of the zinc phosphate coating on the AZ91D magnesium alloy: (a) 1.5 s, (b) energy spectrum of P, (c) energy spectrum of Mg, (d) energy spectrum of Al, (e) energy spectrum of Zn.

time. Fig. 1 (a) shows the surface morphology of the sample immersed in the bath for 1.5 s. Many small crystal nucleus formed uniformly on the surface, which have an average size of 0.2–0.3 μm. It can be calculated that there were 2.1×10^5 crystal nucleus per square centimeter. Such a great number of nucleus distributed equably on the surface of magnesium alloy imply that nucleation should occur uniformly on both α and β phases ($Mg_{17}Al_{12}$) of the magnesium alloy.

In order to prove this, the energy spectrum analysis on the phosphated surface were conducted. Fig. 2 (a) shows the surface morphology (×10,000) of the AZ91D sample immersed in the bath for 1.5 s. And the Energy Spectrum of P, Mg, Al, and Zn are shown in Fig. 2 (b), (c), (d) and (e). By comparing Fig. 2 (a) with the Energy Spectrum of Mg (Fig. 2 (c)) and Al (Fig. 2 (d)), it can be seen that the nucleation formed on not only α phases but also on β phases. By comparing the Energy Spectrum of Zn, Fig. 2 (e), with the Energy Spectrum of P, Fig. 2 (b), (also Mg (Fig. 2 (c)) and Al (Fig. 2 (d)), it is found that zinc particles deposited on both of α and β phases. It is also seen that the density of zinc is higher on some sites (Fig. 2 (e)) of α phases but the P density is not higher on these sites (Fig. 2(b)). Therefore, it can be concluded that there are metallic zinc beside zinc phosphate. It will be proved further by XRD that they are zinc particles.

Hence, some magnesium atoms on α phases dissolved at the micro anodes and other formed MgF rapidly with the F ion in the bath. Some zinc phosphates deposited on the MgF. Some zinc ions were reduced to metallic zinc and were deposited on the MgF because the standard potential of zinc (−1.76 V) is more positive than that of magnesium (−2.36 V). As discussed above, hopeite tends to form on the micro cathode sites of both α phases and β phases. And the metallic zinc forms on the micro the micro cathode sites of α phases.

Fig. 1 (b), (c) and (d) show the growth process of phosphating film at different times of 5, 10 and 30 s, respectively. Some particles grew quickly (or joined together) to form big "white flowers" of sizes about 5–10 μm in 5–30 s. EDS analysis on these regions indicated that these white flowers consist mainly of hopeite. Many other nucleus grew slowly to about 0.5–0.8 μm in 5–30 s. EDS analysis indicated that they were mainly metallic zinc. Because hopeite grew very quickly most substrate was covered by white flowers (hopeite) after phosphatization of 30 s (Fig. 1 (d)). It is seen that there were some clusters of slab-like phosphate crystals after phosphatization of 60 s (Fig. 1(e)). These slabs consisted of hopeite. After phosphatization of 180 s, the surface was fully covered by slab-like phosphate crystals.

Fig. 3 shows the XRD patterns of the specimens with different phosphatization time. It is seen that the phases of phosphate coating are $Zn_3(PO_4)_2 \cdot 4H_2O$ and Zn crystals, which is in agreement with the above discussion on the formation mechanism of phosphate film. A tendency of phosphate crystal growth along (020) direction was observed. The growth process of phosphatization on magnesium alloy could be analyzed by the relative variation of peak intensity of different phases as phosphatization time. Fig. 4 showed the diffraction intensity variations of the (020) plane of hopeite, the (101) plane of zinc
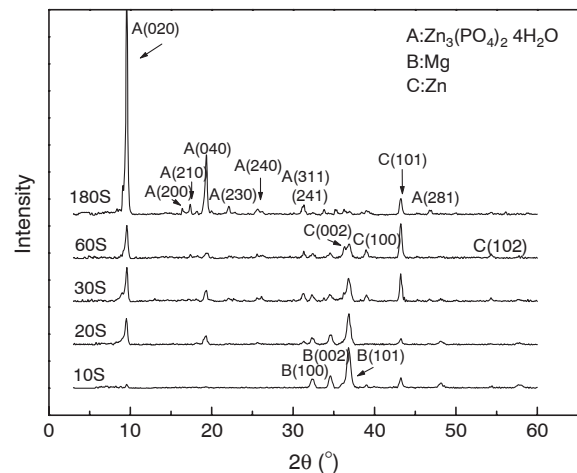

Fig. 3. XRD spectrum of the zinc phosphate coating on the AZ91D magnesium alloy with different immersion times in the phosphating bath.

and the (101) plane of magnesium as phosphatization time, respectively. The continuous decrease of the intensity of the (101) plane of magnesium during the phosphating process indicated the continuous growth of the phosphatization film, which covered the substrate. During the phosphatization time of 0–60 s, both the intensities of the (020) plane of hopeite and the (101) plane of zinc increased, which means that both hopeite and metallic zinc co-deposited on the surface of the magnesium alloy. That is, both the reactions of Eqs. (7) and (9) took place simultaneously. However, after 60 s, the decrease of the intensity of the (101) plane of zinc and the continuous increase of the intensity of the (020) plane of hopeite were observed. This implied that after the magnesium substrate was nearly covered by the phosphate film (see Fig. 3(e)), there is no dissolution of magnesium to insure the deposition of metallic zinc. Therefore, only hopeite deposition maintained. Because there is no small zinc particles to interdict the growth of hopeite, many clusters of large slab-like crystals formed on the surface (Fig. 1(f)).

Fig. 5 (a) and (b) shows the variations of coating weight and open circuit potential during phosphatization, which represent the growth rate of phosphate film. There is a rapid growth period of phosphate film in the initial 30 s. The quick formation of the phosphate film caused the open potential to shift rapidly to the positive direction. Afterwards, because a majority of the substrate was covered by phosphate film, the growth rate of the coating weights tends to slow and the increase of open potential also became slow. In this stage, the phosphate film became dense and there is no gap or crack on the phosphate film.

Fig. 6 shows the polarization curves for the magnesium alloy substrate and the phosphate coatings on the substrate. The cathode reaction in the polarization curve corresponded to the evolution of the hydrogen, and the anodic polarization curve was the most important features related to the corrosion-resistance of the coatings. Current density increases with increasing anodic over-voltage through the entire range of anodic polarization. The corrosion potentials (E_{corr}) of the
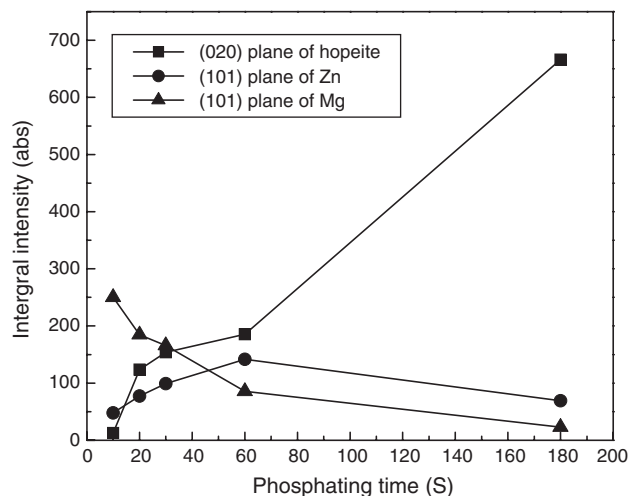
Fig. 4. The variations of the hopeite, Zn and Mg content in the phosphate coating on the AZ91D magnesium alloy with phosphating time and according to XRD spectrum.
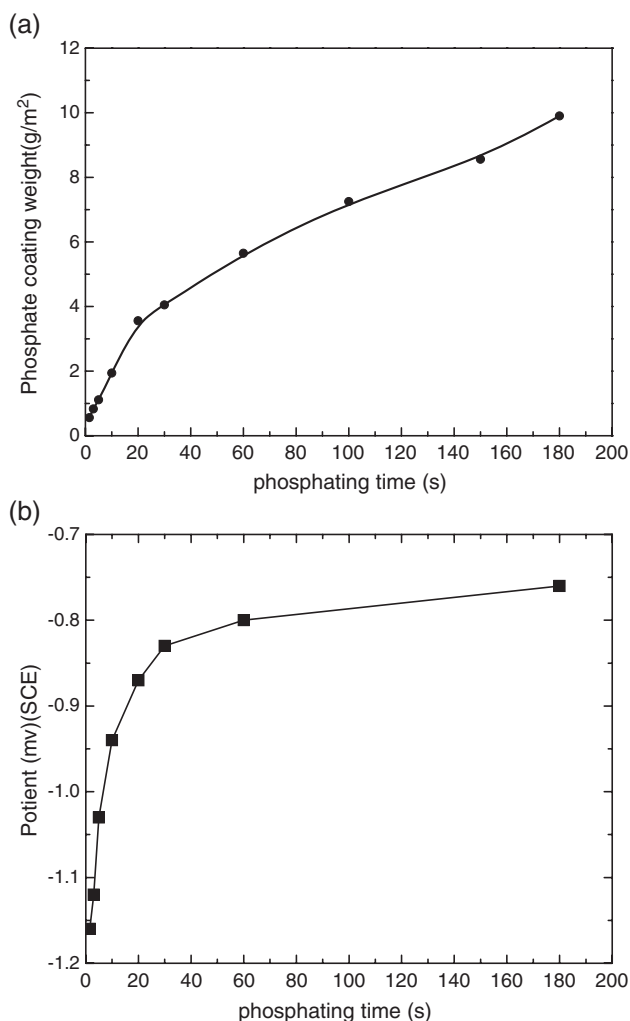

Fig. 6. Polarization curves for the phosphate coating on the AZ91D alloy and the bare AZ91D alloy.

Fig. 5. Phosphate coating weight (a) and open circuit potential (b) increase with immersion time in the phosphating bath.

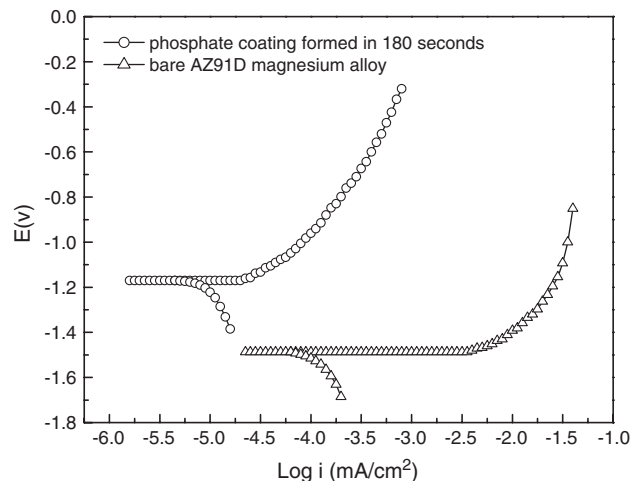coatings shifted positively about 350 mV compared with that of the magnesium alloy substrate. The corrosion current density i_{corr} decreased from about 0.27 mA/cm^2 of the substrate to about 0.02 mA/cm^2 of the coatings. Therefore, the phosphate coatings exhibit lower corrosion rate or higher corrosion resistance than the magnesium alloy substrate, and high corrosion resistance of the phosphate coating will be expected.

4. Conclusions

Zinc phosphate coating was formed on the AZ91D magnesium alloy through a phosphating bath containing mainly ZnO, Zn(NO$_3$)$_2$, H$_3$PO$_4$, NaF, NaClO$_3$. The growth process of phosphate film was investigated through SEM, XRD and EDS.

Some zinc ions were reduced to metallic zinc because the standard potential of zinc is more positive than that of magnesium. Hopeite tends to form on the micro cathode sites of both α phases and β phases. The metallic zinc forms on the micro cathode sites of the α phases.

There were two stages of growth for the phosphate film. At the first stage, the surface of the magnesium alloy divided into micro anode sites (α phases, lower electron density sites) and micro cathode sites (β phase, higher electron density sites). Both the Zn$_3$(PO$_4$)$_2$·4H$_2$O and the metallic zinc deposited on the β and the α phases of the substrate, respectively. After the substrate was nearly covered, the reaction of Zn replacing Mg was impossible, only Zn$_3$(PO$_4$)$_2$·4H$_2$O grew continuously to form slab-like crystals.

The formed zinc phosphate coating exhibited high corrosion resistance in 5% NaCl solution as shown by polarization measurement.

Acknowledgments

References

[1] K. Funatania, Surf. Coat. Technol. l33–l34 (2000) 264.
[2] J.E. Gray, B. Luan, J. Alloys Compd. 336 (2002) 88.
[3] K. Funatania, Surf. Coat. Technol. l33–l34 (2000) 264.
[4] F. Delaunois, J.P. Petitjean, P. Lienard, M. Jacob-Duliere, Surf. Coat. Technol. 124 (2000) 201.
[5] F. Hollstein, R. Wiedemann, J. Scholz, Surf. Coat. Technol. 162 (2003) 261.
[6] L.H. Chiu, C.C. Chen, C.F. Yang, Surf. Coat. Technol. 191 (2005) 181.
[7] D. Hawke, D.L. Albright, Meter. Finish. 10 (1995) 34.
[8] H. Umehara, M. Takaya, S. Terauchi, Surf. Coat. Technol. 69-l70 (2003) 666.
[9] G.Y. Li, L.Y. Niu, J.S. Lian, Z.H. Jiang, Surf. Coat. Technol. l76 (2004) 2l5.
[10] L. Lazzarotto, C. Maréchal, L. Dubar, A. Dubois, J. Oudin, Surf. Coat. Technol. l22 (1999) 94.
[11] A.S. Akhtar, D. Susac, P. Glaze, K.C. Wong, P.C. Wong, K.A.R. Mitchell, Surf. Coat. Technol. l87 (2004) 208.
[12] V. Nelea, V. Craciun, M. Iliescu, I.N. Mihailescu, H. Pelletier, P. Mille, J. Werckmann, Appl. Surf. Sci. 208 (2003) 638.
[13] D. Susac, X. Sun, R.Y. Li, K.C. Wong, P.C. Wong, K.A.R. Mitchell, R. Champaneria, Appl. Surf. Sci. 239 (2004) 45.
[14] L. Kouisni, M. Azzi, M. Zertoubi, F. Dalard, S. Maximovitch, Surf. Coat. Technol. l85 (2004) 58.
[15] L.Y. Niu, Z.H. Jiang, G.Y. Li, C.D. Gu, J.S. Lian, Surf. Coat. Technol. 200 (2006) 3021.
[16] R. Ambat, N.N. Aung, W. Zhou, Corros. Sci. 42 (2000) l433.
[17] G.L. Song, A. Atrens, X.L. Wu, B. Zhang, Corros. Sci. 40 (1998) 1769.